

Fabrication and characterization of $\text{Ge}_{20}\text{Sb}_{15}\text{S}_{65}$ chalcogenide glass for photonic crystal fibers

Changshen Yi · Peiqing Zhang · Feifei Chen ·
Shixun Dai · Xunsi Wang · Tiefeng Xu ·
Qihua Nie

Received: 2 November 2013 / Accepted: 9 December 2013 / Published online: 13 February 2014
© Springer-Verlag Berlin Heidelberg 2014

Abstract Chalcogenide glasses are known for their high transparency in the mid-infrared (IR) range, which includes two atmospheric windows that lie from 3 to 5 μm and 8 to 12 μm , respectively. Chalcogenide photonic crystal fibers have numerous potential applications in the field of IR, such as spectroscopy, microscopy, astronomy, biology, and sensing. In this paper, $\text{Ge}_{20}\text{Sb}_{15}\text{S}_{65}$ chalcogenide glass was fabricated and systematically studied. Chalcogenide glass has high transmission property ($>70\%$), good thermal stability, and good mechanical stability. The glass transition temperature T_g is 296 $^{\circ}\text{C}$, and no exothermic peak was associated with crystallization up to 500 $^{\circ}\text{C}$, which indicates its suitability for fiber drawing. As a result of its excellent mechanical properties, preforms with a variety of geometrical patterns were fabricated by using mechanical drilling. The near-field intensity distribution image of the drawn fiber shows a strong light propagation confinement.

1 Introduction

Photonic crystal fibers (PCFs), which are also called microstructured or holey fibers, have many unique properties

that are unobtainable in conventional fibers [1, 2]. PCFs have highly adjustable mode field diameters (MFDs). Large MFDs are useful for minimizing the risk of glass damage during high-power laser propagation, whereas small MFDs enable the enhancement of nonlinear effects [3]. An index-guiding PCF can be set as an endless single mode [4] regardless of the small size of the wavelength of light. Chromatic dispersion can easily be managed in PCF by tailoring waveguide dispersion. Potential applications of PCFs, which initially included telecommunications, have now been extended to include spectroscopy, metrology, microscopy, astronomy, micromachining, biology, and sensing [5, 6].

At present, the main background materials of the researched PCFs are oxide-based glasses, including silica and heavy oxide glasses. Unlike oxide-based glasses, chalcogenide glasses can be transparent from the visible region (sulfur-based glass) up to the mid-infrared region (25 μm for telluride glasses). As a good infrared material, chalcogenide glasses offer very high refractive indices (2.0–3.5) and very low phonon energies (down to 350 cm^{-1}), which is beneficial for producing photonic devices. Another remarkable property of chalcogenide glasses is their high optical nonlinearity. The nonlinear refractive index of sulfur-based glasses is more than 100 times higher than that of silica and can be 1,000 times higher than that of silica for selenium- and tellurium-based glasses [7, 8]. In addition to their excellent optical properties, chalcogenide glasses have good thermal and mechanical stability, and have been successfully drawn into optical fibers during the last 10 years. A chalcogenide PCF was first proposed in 2000 [9], but the fabricated PCFs did not exhibit any light guidance. Since then, various chalcogenide PCFs with different core diameter and acceptable losses have been demonstrated [10–12].

C. Yi · P. Zhang · F. Chen · S. Dai (✉) · X. Wang · T. Xu ·
Q. Nie
Infrared Materials and Devices Laboratory of Ningbo University,
Ningbo University, Ningbo 315211, Zhejiang, China
e-mail: daishixun@nbu.edu.cn

P. Zhang
e-mail: zhangpeiying@nbu.edu.cn

P. Zhang
State Key Laboratory of Optoelectronic Materials and
Technologies, Sun Yat-sen University,
Guangzhou 510275, Guangdong, China

Currently, the development of PCFs in the mid-infrared range is of great interest for applications such as laser power transmission in atmospheric windows of 3–5 and 8–12 μm , and in infrared supercontinuum generation, among others.

Two main techniques have been used to fabricate chalcogenide glass MOFs. The first one is the capillary-stacking technique, which is commonly used to manufacture silica PCFs and is also widely used for the fabrication of chalcogenide glass PCFs [13–15]. This technique can produce microstructured preforms with highly complex periodic geometry (> 60 holes), but necessitates a huge amount of tricky handling. The second technique is extrusion, which is easier to perform than capillary stacking. However, extrusion is still quite challenging when used to produce preforms with very complex microstructure patterns, such as a triangular holey structure with more than three rings of air holes [16].

In this study, $\text{Ge}_{20}\text{Sb}_{15}\text{S}_{65}$ chalcogenide glass was fabricated and systematically studied. Results showed $\text{Ge}_{20}\text{Sb}_{15}\text{S}_{65}$ chalcogenide glass has high transmission and good thermal stability, which can be introduced into PCFs for mid-infrared applications. The prepared glass has excellent mechanical properties. Therefore, a mechanical drilling method was developed to fabricate PCF preforms with a variety of geometrical patterns. Because the viscosity value is not available, PCF preforms were drawn at different temperatures, namely, 430, 435, and 465 $^{\circ}\text{C}$. After each drawing, X-ray diffraction (XRD) was performed on the drawn PCF to confirm whether crystallization occurred during fiber drawing at those temperatures. We also observed the near-field intensity distribution of the drawn fiber by using a microscope objective and a CCD camera.

2 Glass synthesis and properties of glass

2.1 Glass synthesis

Glasses used in optical devices require meticulous synthesis. Chalcogenide glasses are prepared with highly pure raw materials (5 N) in silica ampoules under vacuum (10^{-3} bar). The starting materials are distilled in different tubes, and sulfur is thoroughly purified by performing multiple distillations to eliminate water and carbon, which hinder the transmission of glasses. After purification, required amounts of the different elements are placed in the same silica ampoules with a 20 mm diameter. Ampoules were sealed while being continuously evacuated. The sealed ampoules were then melted by using a rocking furnace at 950 $^{\circ}\text{C}$ for 10 h and then cooled to 650 $^{\circ}\text{C}$ for 1 h. Finally, the ampoules were quenched in ice water to

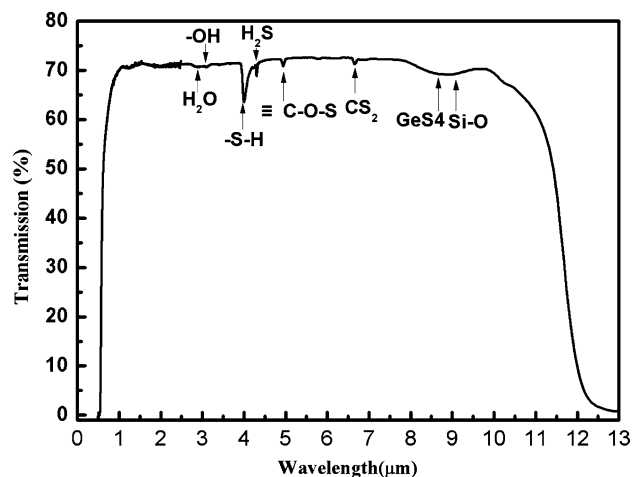


Fig. 1 Transmission spectra of chalcogenide glass $\text{Ge}_{20}\text{Sb}_{15}\text{S}_{65}$ in the range of 0.5–13 μm

allow glass formation and to avoid crystallization. Afterward, the vitreous sample was annealed at a temperature slightly below the glass transition temperature ($T_g - 10$ $^{\circ}\text{C}$) before being slowly cooled to room temperature.

All optical tests were performed at room temperature. The glasses are cut into 2-mm thick disks, and their two parallel sides were polished carefully to prepare them for the measurement of their thermal and optical properties.

2.2 Properties of glass

The IR transparency spectrum was measured by using a PerkinElmer-Lambda 950 UV/VIS/NIR spectrophotometer over a spectral range from 400 to 2,500 nm and Fourier transform infrared spectroscopy (Thermo Nicolet, Nexus 380, USA) over the range of 2.5–25 μm at room

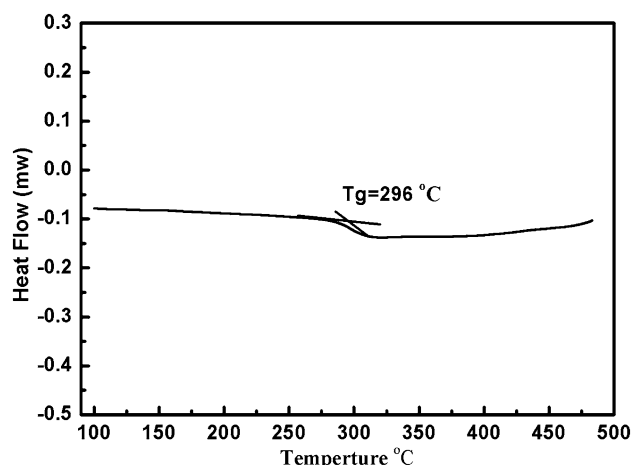


Fig. 2 DSC curve of glass $\text{Ge}_{20}\text{Sb}_{15}\text{S}_{65}$. No exothermic peaks associated with crystallization up to 500 $^{\circ}\text{C}$ can be observed

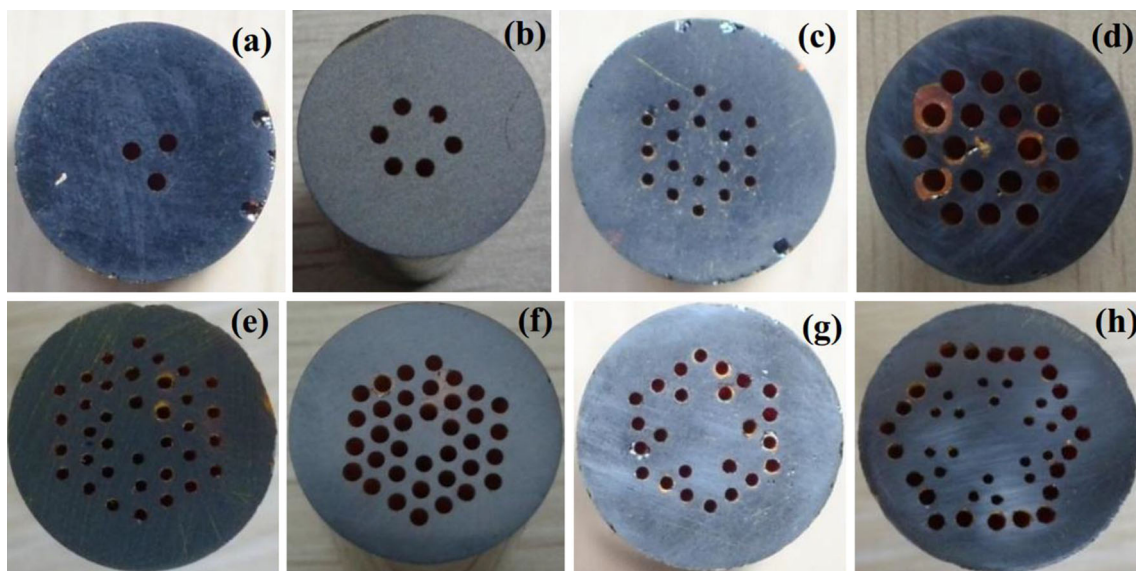


Fig. 3 PCF preforms produced by mechanical drilling: **a, b** 3- and 6-air-hole preforms for suspended core fibers; **c, d** 18-air-hole preforms; **e, f** 36-air-hole preforms; **g, h** 24- and 52-air-hole preforms designed for photonic crystal fibers with a large area

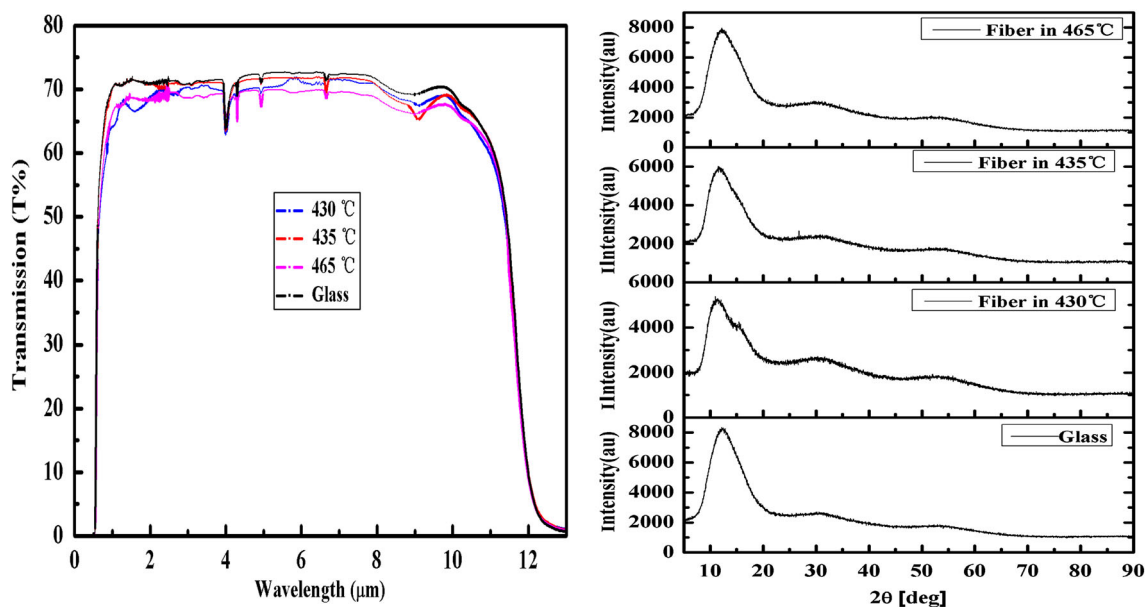


Fig. 4 **a** Transmission and **b** XRD of Ge₂₀Sb₁₅S₆₅ glasses that are thermally handled at 430, 435, and 465 °C

temperature. The transmission curve of the fabricated Ge₂₀Sb₁₅S₆₅ glass is presented in Fig. 1. The transmittance of the sample in the range of 1–10 μm exceeds 70 % except for some absorption bands, which indicates excellent optical quality for photonic devices. The related absorption bands are also identified according to the previous experimental results [17]. As indicated in Fig. 1, the absorption bands at 4.9, 6.6, 8.7, and 9.1 μm are ascribed to the vibration of ≡ C–O–S, CS₂, GeS₄, and Si–O bonds,

respectively. These impurity bands are caused by pollution of the initial raw materials. Therefore, the absorption intensity of these impurity bands can be alleviated by multiple distillations.

Whether a glass material can be drawn into an optical fiber is mainly related to its thermal stability. The thermal properties of the glass were studied by performing differential scanning calorimetry (DSC) at a heat rate of 10 °C/min (PerkinElmer Pyris Diamond), as shown in Fig. 2.

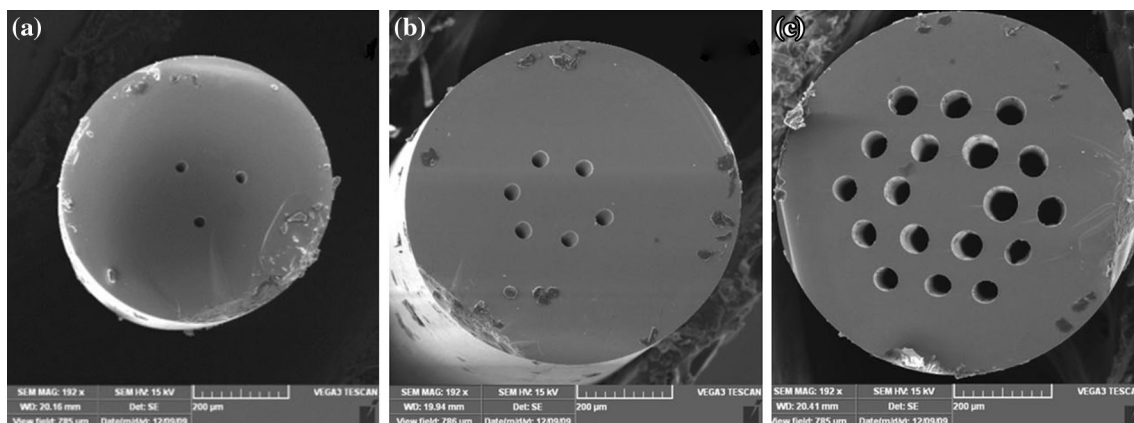


Fig. 5 Geometrical profiles of photonic crystal fibers drawn from preforms depicted in Fig. 4 (PCFs **a**, **b**, **c** correspond to preforms **a**, **b**, **d**, respectively)

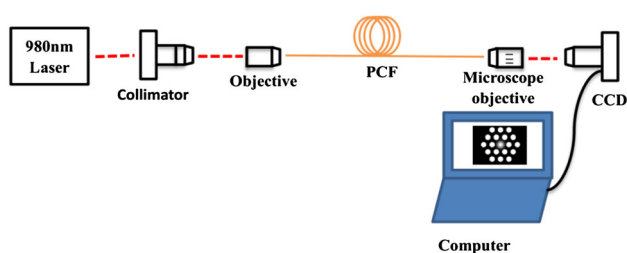


Fig. 6 Chalcogenide PCF output beam imaging setup

Glass with a transition temperature of $T_g = 296\text{ }^\circ\text{C}$ is usable for temperatures that exceed $200\text{ }^\circ\text{C}$. In addition, no exothermic peak associated with crystallization up to $500\text{ }^\circ\text{C}$ was observed, which indicates that this glass is thermally and dynamically stable toward devitrification. Furthermore, glass with a $\Delta T = T_g - T_x$ (T_x is the temperature of crystallization onset) higher than $100\text{ }^\circ\text{C}$ is suitable for fiber drawing. Therefore, the $\text{Ge}_{20}\text{Sb}_{15}\text{S}_{65}$ glass is suited for PCF applications.

The mechanical strength of the glass is an important factor in the fabrication of PCF preforms by using mechanical drilling, especially for preforms that have a series of air holes located on a hexagonal or octagonal lattice. Microhardness is the mechanical strength of glasses and determines the extent of the flaws and the durability of the fiber, which is measured with a charge of 25 g for 5 s by using a Vickers microindenter (Everone MH-3, Everone Enterprise Ltd., Shanghai, China). The hardness is obtained by the equation $HV = 1.8544 \times Q/d^2$, where Q and d denote the exerted load and the average diameter of diamond prism indentation in glass, respectively. The average hardness of the glass is 210.1 kg mm^{-2} , higher than that of glasses in the Ref. [18], which indicates that the prepared glass has excellent mechanical properties.

3 Photonic crystal fiber preforms and fiber drawing

Drilling techniques have been successfully used to prepare preforms, such as ultrasonic drilling for glasses or mechanical drilling for polymers. In this study, we developed mechanical drilling equipment for the preparation of chalcogenide glasses preforms with a variety of geometrical patterns. Not all chalcogenide glasses can be created into preforms by performing mechanical drilling, because some of them are very fragile. Fortunately, as described above, our fabricated glasses are strong enough to be drilled into fiber preforms with complex geometrical patterns. The drilling device that we designed and manufactured consists of two main parts: a broach for drilling and a precise x - y platform for position control of air holes. We also introduced a water cooling system to eliminate heat generated by friction between the glass and the broach during drilling to avoid gradual embrittlement of the glass rod. When the drilling process is finished, the inner surface of the air holes was further polished by using a special broach, which is critical for ensuring the quality of the subsequently drawn fiber. Through optimization of the drilling parameters, especially rotation speed, applied force, and cooling rate, a variety of complex PCF structures that feature regular or irregular air-hole patterns in a glass rod can be fabricated. Experiment results have shown that some PCF structures with closely spaced air holes can be obtained, which validates the excellent mechanical stability of our prepared glasses.

Figure 3 shows PCF preforms manufactured by using mechanical drilling. These preforms had an outer diameter of 18 mm , and the diameters of the air holes range from 0.8 to 2 mm . The air-hole ratio d/Λ can also be different and range from 0.4 to 0.625 , which indicates that the holes are closely spaced. Figure 3a, b show the simplest PCF structures, with three air holes and six air holes arranged in a ring, respectively. PCFs with these structures have weak

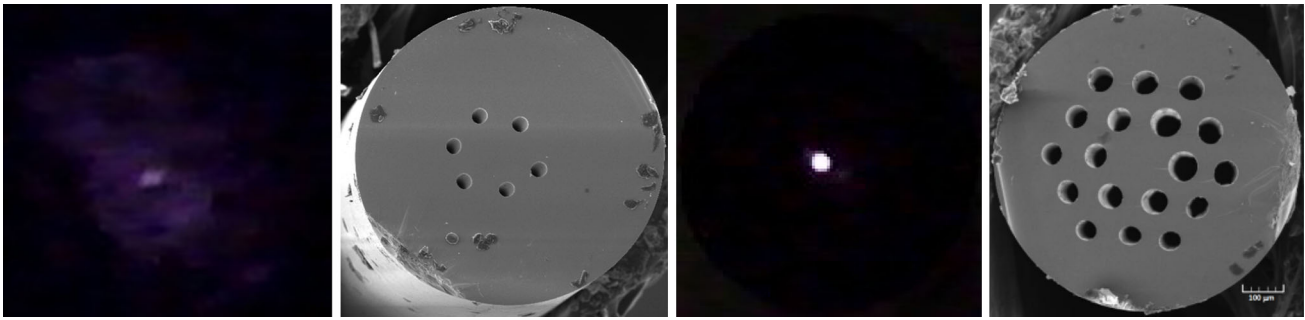


Fig. 7 Near-field imaging at 0.98 μm for the two PCFs

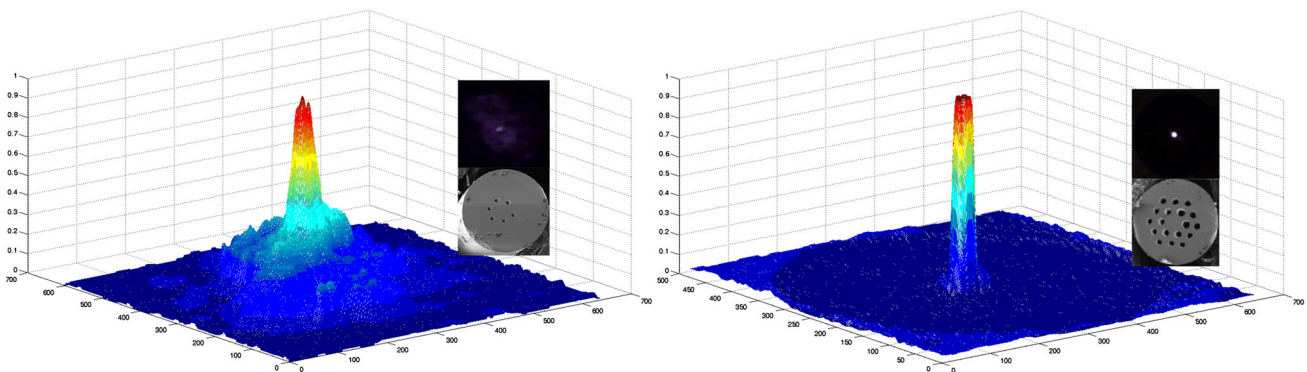


Fig. 8 Near-field intensity distribution of PCFs visualized in 3-D

laser beam propagation ability. However, these preforms can be made into suspended core fibers for nonlinear optical applications by enhancing pressure in the air holes during fiber drawing [19]. Figure 3c, d show PCF preforms with 18 air holes arranged in two rings with different air filling ratios. These structures are relatively easy to fabricate, but both can work in single mode with acceptable losses. The loss of the PCF can be significantly reduced by increasing the air-hole rings, such as the structure shown in Fig. 3e, f. We also prepared complex preforms for PCFs with ultralarge mode areas, as shown in Fig. 3g, h which can be applied to high-powered laser propagation and fiber amplifiers [20].

The preforms were then drawn into PCF with a fiber drawing tower (TGL-A, China). The properties of chalcogenide glasses are significantly different from those of traditional oxide glasses. Therefore, the drawing parameters must be carefully controlled during PCF drawing, such as temperature curve, translation speed, fiber drawing speed, and pressure in the holes, among others.

In the drawing process, a suitable temperature is the key parameter to obtain a fiber without crystallization. As discussed above, the glass transition temperature T_g is 296 °C, with no exothermic peak associated with crystallization up to 500 °C. Fibers can be drawn at any temperature between 296 and 500 °C. However, glass viscosity

is another parameter that must be considered. In general, fiber drawing is performed on the condition that glass viscosity is between 10^4 and 10^5 pa.s [21, 22]. Deriving the optimal viscosity based on the temperature is difficult. Therefore, we attempted to perform drawing at different temperatures that range from 296 to 500 °C. We observed that fiber drawing at temperatures lower than 430 °C is not optimal because glass viscosity at this temperature is too high, which prevents drawing from being performed smoothly. PCF preforms have been successfully drawn at 430, 435, and 465 °C. Drawing results show that PCFs drawn at 465 °C exhibited the most strongly collapsed air holes because of the liquidity of glass. PCFs drawn at 430 °C have perfect air holes around the core. Transmission and XRD of waste materials from fiber drawing at 430, 435, 465 °C were studied, which are shown in Fig. 4. Compared with the glass without drawing, the transmission property of drawn materials varied slightly. XRD analysis also showed that preforms drawn below 465 °C are still in the amorphous state, which confirms the thermal stability of the prepared Ge₂₀Sb₁₅S₆₅.

Selecting suitable sets of parameters obtained various types of chalcogenide PCFs. Figure 5 shows cross sections of several PCFs that were drawn from the preforms obtained by using mechanical drilling. The microscopic structures of the PCFs in Fig. 5 are uniform.

4 Propagation property of photonic crystal fibers

The experiment setup for the propagation measurement of the drawn PCFs is shown in Fig. 6. The output of the laser with a central wavelength set at 980 nm was first collimated by using a collimator and then coupled into the PCF by using an objective. A microscope and a CCD detector were used to monitor the intensity distribution in the end cross section of the fiber. The observed near-field optical image of the PCFs is shown in Fig. 7. Figure 8 shows the reconstructed 3-D profile of the intensity distribution of the PCFs. It is shown that most of the injected optical energy was confined to the core of the PCFs, especially for the 18-air-hole PCF. Moreover, the effective mode area of the 18-air-hole PCF is roughly estimated as $1,962 \mu\text{m}^2$, which can reduce transmissive optical power density and therefore increase the nonlinearity threshold of the PCF. Furthermore, the prepared PCFs in this study are all bare fibers without any coating. Previous studies indicate that fibers coated with absorbing gallium/indium on the surface prevent the propagation of any residual signals in the cladding (cladding modes) [23, 24], which can improve the measured effect of near-field intensity distribution. Therefore, the propagation quality of our prepared PCFs is expected to improve with the introduction of some absorbing coatings.

5 Conclusion

$\text{Ge}_{20}\text{Sb}_{15}\text{S}_{65}$ chalcogenide glass was fabricated and systematically studied by the transmission, DSC, XRD, and microhardness. The results show that $\text{Ge}_{20}\text{Sb}_{15}\text{S}_{65}$ chalcogenide glasses have excellent optical quality, good thermal stability, and excellent mechanical stability. PCF preforms with a variety of geometrical patterns were fabricated by using the developed mechanical drilling equipment. Fiber drawing techniques were also studied. High-quality PCFs were successfully drawn by optimizing the drawing temperature, translation speed, fiber drawing speed, and pressure. Strong light propagation confinement in the fiber was observed by using a microscope objective and a CCD camera. The profile of the near-field intensity image shows that the prepared PCF can work with a large mode area, which is important in high-power laser propagation and fiber amplifiers.

Acknowledgments The work was supported by National Program on Key Basic Research Project (973 Program) (No. 2012CB722703), the National Natural Science Foundation of China (Nos. 61177087, and 61307060), Zhejiang Provincial Natural Science Foundation of China (No. LQ12F05004), Program for Innovative Research Team of Ningbo City (No. 2009B21007), Natural Science Foundation of Ningbo City (2012A610116), Program for New Century Excellent

Talents in University (NCET-10-0976), Project of Optoelectronic Materials and Technologies State Key Laboratory and K. C. Wong Magna Fund in Ningbo University.

References

1. J.C. Knight, T.A. Birks, P.S.J. Russell, D.M. Atkin, *Opt. Lett.* **21**, 1547 (1996)
2. I. Abdelaziz, H. Ademgil, F. AbdelMalek, S. Haxha, T. Gorman, H. Bouchriha, *Opt. Commun.* **283**, 5218 (2010)
3. T.M. Monro, D.J. Richardson, *C.R. Phys.* **4**, 175 (2003)
4. T.A. Birks, J.C. Knight, P.S.J. Russell, *Opt. Lett.* **22**, 961 (1997)
5. J.C. Knight, *Nature* **424**, 847 (2003)
6. P. Russell, *Science* **299**, 358 (2003)
7. J.S. Sanghera, C.M. Florea, L.B. Shaw, P. Pureza, V.Q. Nguyen, M. Bashkansky, Z. Dutton, I.D. Aggarwal, *J. Non-Cryst. Solids* **354**, 462 (2008)
8. L. Petit, N. Carlie, K. Richardson, A. Humeau, S. Cherukulappurath, G. Boudebs, *Opt. Lett.* **31**, 1495 (2006)
9. T.M. Monro, Y.D. West, D.W. Hewak, N.G.R. Broderick, D.J. Richardson, *Electron. Lett.* **36**, 1998 (2000)
10. L. Brilland, F. Smektala, G. Renversez, T. Chartier, J. Troles, T. Nguyen, N. Traynor, A. Monteville, *Opt. Express* **14**, 1280 (2006)
11. Q. Coulombier, L. Brilland, P. Houizot, T. N. N'Guyen, T. Chartier, G. Renversez, A. Monteville, J. Fatome, F. Smektala, T. Pain, H. Orain, J. C. Sangleboeuf, J. Trolès, in *Fabrication of low losses chalcogenide photonic crystal fibers by molding process*, (2010)
12. C. Conseil, Q. Coulombier, C. Boussard-Plédel, J. Troles, L. Brilland, G. Renversez, D. Mechin, B. Bureau, J. Adam, J. Lucas, *J. Non-Cryst. Solids* **357**, 2480 (2011)
13. F. Smektala, F. Desevedavy, L. Brilland, P. Houizot, J. Troles, and N. Traynor, 658803 (2007)
14. F. Désévéday, G. Renversez, L. Brilland, P. Houizot, J. Troles, Q. Coulombier, F. Smektala, N. Traynor, J.-L. Adam, *Appl. Opt.* **47**, 6014 (2008)
15. F. Désévéday, G. Renversez, J. Troles, L. Brilland, P. Houizot, Q. Coulombier, F. Smektala, N. Traynor, J.-L. Adam, *Appl. Opt.* **48**, 3860 (2009)
16. X. Feng, A.K. Mairaj, D.W. Hewak, T.M. Monro, *J. Lightwave Technol.* **23**, 2046 (2005)
17. Y. Li, C. Lin, Z. Li, F. Wang, *J. Optoelectron. Adv. Mater.* **14**, 717 (2012)
18. L. Ying, C. Lin, Q. Nie, Z. Li, Y. Xu, F. Chen, S. Dai, *J. Am. Ceram. Soc.* **95**, 1320 (2012)
19. M. El-Amraoui, J. Fatome, J.-C. Jules, B. Kibler, G. Gadret, C. Fortier, F. Smektala, I. Skripatchev, C. Polacchini, Y. Messaddeq, *Opt. Express* **18**, 4547 (2010)
20. C.S. Yi, P.Q. Zhang, X.S. Wang, X. Shen, T.F. Xue, Q.H. Nie, *Acta Phys. Sin* **62**, 84206 (2013)
21. A.B. Seddon, Z. Tang, D. Furniss, S. Sujecki, T.M. Benson, *Opt. Express* **18**, 26704 (2010)
22. G. Yang, T. Rouxel, J. Troles, B. Bureau, C. Boussard-Plédel, P. Houizot, J.C. Sangleboeuf, *J. Am. Ceram. Soc.* **94**, 2408 (2011)
23. S. Mauriceon, C. Boussard-Plédel, J. Troles, A.J. Faber, P. Lucas, X.H. Zhang, J. Lucas, B. Bureau, *J. Lightwave Technol.* **28**, 3358 (2010)
24. M. El-Amraoui, G. Gadret, J.C. Jules, J. Fatome, C. Fortier, F. Désévéday, I. Skripatchev, Y. Messaddeq, J. Troles, L. Brilland, W. Gao, T. Suzuki, Y. Ohishi, F. Smektala, *Opt. Express* **18**, 26655 (2010)